

A NEW INTERPRETATION FOR THE SECOND PEAK OF T CORONAE BOREALIS OUTBURSTS: A TILTING DISK AROUND A VERY MASSIVE WHITE DWARF

IZUMI HACHISU

Department of Earth Science and Astronomy, College of Arts and Sciences, University of Tokyo, Komaba,
 Meguro-ku, Tokyo 153-8902, Japan; hachisu@chianti.c.u-tokyo.ac.jp

AND

MARIKO KATO

Department of Astronomy, Keio University, Hiyoshi, Kouhoku-ku, Yokohama 223-8521, Japan;
 mariko@educ.cc.keio.ac.jp

to be published in the Astrophysical Journal, Letters

ABSTRACT

A new interpretation for the second peak of T Coronae Borealis (T CrB) outbursts is proposed based on a thermonuclear runaway (TNR) model. The system consists of a very massive white dwarf (WD) with a tilting accretion disk and a lobe-filling red-giant. The first peak of the visual light curve of T CrB outbursts is well reproduced by the TNR model on a WD close to the Chandrasekhar mass ($M_{WD} \gtrsim 1.35 M_{\odot}$), while the second peak is reproduced by the combination of the irradiated M-giant and the irradiated tilting disk. The derived fitting parameters are the WD mass $M_{WD} \sim 1.35 M_{\odot}$, the M-giant companion mass $M_{RG} \sim 0.7 M_{\odot}$ ($0.6 - 1.0 M_{\odot}$ is acceptable), the inclination angle of the orbit $i \sim 70^\circ$, and the tilting angle of the disk $i_{\text{prec}} \sim 35^\circ$. These parameters are consistent with the recently derived binary parameters of T CrB.

Subject headings: accretion disks — binaries: close — binaries: symbiotic — novae — stars: individual (T CrB)

1. INTRODUCTION

T Coronae Borealis (T CrB) is one of the well observed recurrent novae and characterized by a secondary, fainter maximum occurring ~ 100 days after the primary peak. Historically, T CrB bursted twice, in 1866 and 1946, with the light curves very similar each other (e.g., Pettit 1946d). Large ellipsoidal variations in the optical light curves during quiescent phase suggest that an M3–4 red-giant component fills its Roche lobe (e.g., Leibowitz et al. 1997; Shahbaz et al. 1997; Belczyński & Mikolajewska 1998). There have been debates on the nature of the hot component of this binary system. Webbink (1976) and Webbink et al. (1987) proposed an outburst mechanism of T CrB based on their main-sequence accretor model. This accretion event model was investigated further by 3D numerical simulations (Cannizzo & Kenyon 1992; Ruffert et al. 1993).

However, Selvelli, Cassatella, & Gilmozzi (1992) have been opposed to the main-sequence accretor model from their analysis of *IUE* data in its quiescent state, which indicates the existence of a mass-accreting white dwarf (WD). The detection of X-rays and the presence of flickering in the optical light curves are also naturally explained in terms of accretion onto a WD. Their estimated mass accretion rate in quiescent state is very high ($\dot{M}_{\text{acc}} \sim 2.5 \times 10^{-8} M_{\odot} \text{ yr}^{-1}$) and is exactly required by the thermonuclear runaway (TNR) theory to produce a TNR event every 80 yr on a massive ($\gtrsim 1.3 M_{\odot}$) WD. Thus, the 1866 and 1946 outbursts can be interpreted in terms of a TNR event on a very massive WD.

Rapid decline rates of the light curves indicate a very massive WD close to the Chandrasekhar limit, $M_{WD} \sim 1.37 - 1.38 M_{\odot}$ (Kato 1995, 1999). Assuming solar composition of the WD envelope, Kato calculated nova light

curves for WD masses of 1.2, 1.3, 1.35 and $1.377 M_{\odot}$ and found that the light curve of the $1.377 M_{\odot}$ model is in better agreement with the observational light curve of T CrB than the other lower mass models.

Recently, other observational supports for a massive WD in T CrB have been reported. Belczyński and Mikolajewska (1998) derived a permitted range of binary parameters, $M_{WD} = 1.2 \pm 0.2 M_{\odot}$, from amplitude of the ellipsoidal variability and constraints from the orbital solution of M-giants. In Shahbaz et al. (1997), a massive WD of $M_{WD} = 1.3 - 2.5 M_{\odot}$ is suggested from the infrared light curve fitting. Combining these two permitted ranges of the WD mass in T CrB, we may conclude that a mass of the WD is between $M_{WD} = 1.3 - 1.4 M_{\odot}$, which is very consistent with the light curve analysis $M_{WD} \sim 1.37 - 1.38 M_{\odot}$ by Kato (1999).

The secondary maximum in outbursts is not generally observed in classical novae or in other recurrent novae. Selvelli et al. (1992) suggested a possibility of irradiation by a stationary shell around the system, although the presence of the shell is just a speculation. In this Letter, we propose another possibility of the second peak: irradiation by a tilting accretion disk around a massive WD.

The main results of our analysis are: 1) the first peak is naturally reproduced by the fast developing photosphere of the WD envelope based on the TNR model incorporated with a very massive WD ($M_{WD} \sim 1.35 M_{\odot}$). 2) the second peak is not fully reproduced by an irradiated M-giant model as simply estimated by Webbink et al. (1987); 3) the second peak can be well reproduced if we introduce an irradiated tilting accretion disk around the WD in addition to the irradiated M-giant companion. Such tilting instabilities of an accretion disk have been suggested by Pringle (1996) for central stars as luminous as the Eddington limit or more (radiation-induced instability). Because

the maximum luminosity of T CrB outbursts exceeds the Eddington limit (e.g., Selvelli et al. 1992), the radiation-induced instability may work well in T CrB outbursts.

2. THEORETICAL LIGHT CURVES

Our model is graphically shown in Figure 1. The visual light is contributed to by three components of the system: 1) the WD photosphere, 2) the M-giant photosphere, and 3) the accretion disk surface.

2.1. Decay Phase of Novae

In the TNR model, WD envelopes expand greatly as large as $\sim 100 R_\odot$ or more and then the photospheric radius gradually shrinks to the original size of the white dwarfs (e.g., $\sim 0.004 R_\odot$ for $M_{\text{WD}} = 1.35 M_\odot$). The optical luminosity reaches its maximum at the maximum expansion of the photosphere and then gradually darkens to the level in quiescent phase. Since the WD envelopes reach a steady-state in the decay phase of novae (e.g., Kato & Hachisu 1994), we are able to treat the development of the envelope by a unique sequence of steady-state solutions with different envelope masses (ΔM) as shown by Kato & Hachisu (1994).

We have calculated such sequences for WDs with various masses of $M_{\text{WD}} = 0.6, 0.7, 0.8, 0.9, 1.0, 1.1, 1.2, 1.3, 1.35$ and $1.377 M_\odot$ and obtained the optical light curves for the decay phase of TNR events. Here, we choose $1.377 M_\odot$ as a limiting mass just below the mass at the SN Ia explosion in W7 ($1.378 M_\odot$, Nomoto et al. 1984). We have used the updated OPAL opacity (Iglesias & Rogers 1996), which has a strong peak near $\log T \sim 5.2$ about 20 – 30% larger than that of the original OPAL opacity (Rogers & Iglesias 1992) which was used in Kato & Hachisu (1994). The numerical method and various assumptions are the same as those in Kato & Hachisu (1994). It should be noted here that optically thick winds blow when the WD envelope expands and the photospheric temperature decreases below $\log T_{\text{ph}} \sim 5.5$.

Each wind solution is a unique function of the envelope mass ΔM if the WD mass is given. The envelope mass is decreasing due to the wind mass loss at a rate of $\dot{M}_{\text{wind}}(\Delta M)$ and hydrogen shell burning at a rate of $\dot{M}_{\text{nuc}}(\Delta M)$, i.e.,

$$\frac{d}{dt} \Delta M = \dot{M}_{\text{acc}} - \dot{M}_{\text{wind}} - \dot{M}_{\text{nuc}}, \quad (1)$$

where \dot{M}_{acc} is the mass accretion rate to the WD. Integrating equation (1), we follow the development of the envelope mass ΔM and obtain physical quantities such as the photospheric temperature T_{ph} , photospheric radius R_{ph} , photospheric velocity v_{ph} , wind mass loss rate \dot{M}_{wind} , and nuclear burning rate \dot{M}_{nuc} . When the envelope mass decreases to below the critical mass, the wind stops and after that the envelope mass is decreased only by nuclear burning.

2.2. White Dwarf Photosphere

We have assumed a black-body photosphere of the white dwarf envelope. After the optical peak, the photosphere shrinks with the envelope mass being blown off in the wind, and the photospheric temperature increases with

the visual light decrease because the main emitting region moves blueward. Based on our wind solutions, we have obtained visual magnitude of the WD photosphere with a window function given by Allen (1973). The photospheric surface is divided into 16 pieces in the latitudinal angle ($\Delta\theta = \pi/16$) and into 32 pieces in the longitudinal angle ($\Delta\phi = 2\pi/32$) as shown in Figure 1. Then, the contribution of each piece is summed up by considering the inclination angle to the viewer. A linear limb-darkening law (the coefficient is $x = 0.95$, see Belczyński & Mikolajewska 1998; Wilson 1990) is incorporated into the calculation.

2.3. Companion M-giant Photosphere

To construct a light curve, we have also included the contribution of the companion star irradiated by the WD photosphere. The surface of the companion star is assumed to fill the inner critical Roche lobe as shown in Figure 1. Numerically dividing the latitudinal angle into 32 pieces ($\Delta\theta = \pi/32$) and the longitudinal angle into 64 pieces ($\Delta\phi = 2\pi/64$), we have also summed up the contribution of each area considering the inclination angle to the viewer by assuming the same limb-darkening law as the WD photosphere, but we neglect the gravity-darkening effect of the companion star because the hemisphere to the WD is heated up by the irradiation. Here, we assume that 50% of the absorbed energy is reemitted from the hemisphere of the companion with a black-body spectrum at a local temperature. The original (non-irradiated) photospheric temperature of the companion star is assumed to be $T_{\text{ph,RG}} = 3500$ K (Belczyński & Mikolajewska 1998). If the accretion disk around the WD blocks the light from the WD photosphere, it makes a shadow on the surface of the companion star. Such an effect is also included in our calculation.

The orbit of the companion star is assumed to be circular. The light curves are calculated for five cases of the companion mass, i.e., $M_{\text{RG}} = 0.6, 0.7, 0.8, 0.9$, and $1.0 M_\odot$, as derived by Belczyński & Mikolajewska (1998). Since we obtain similar light curves for all of these five masses, we show here only the results for $M_{\text{RG}} = 0.7 M_\odot$. In this case, the separation is $a = 199.3 R_\odot$, the effective radius of the inner critical Roche lobe for the WD component is $R_1^* = 87.0 R_\odot$, the effective radius of the M-giant companion star is $R_2 = R_2^* = 64.5 R_\odot$.

2.4. Accretion Disk Surface

We have included the luminosity coming from the accretion disk irradiated by the WD photosphere when the accretion disk reappears a few to several days after the optical maximum. The surface of the accretion disk absorbs photons and reemits in the same way as the companion does. Here, we assume that the accretion disk surface emits photons as a black-body at a local temperature of the heated surface. We assume further that 25% of the absorbed energy is emitted from the surface, while the other is carried into interior of the accretion disk and eventually brought into the WD. The temperature of the outer edge is assumed to be $T_{\text{disk}} = 2000$ K, which is never irradiated by the WD photosphere.

An axisymmetric accretion disk with a thickness given by

$$h = \beta R_{\text{disk}} \left(\frac{\varpi}{R_{\text{disk}}} \right)^2, \quad (2)$$

is assumed, where h is the height of the surface from the equatorial plane, ϖ the distance on the equatorial plane from the center of the WD, R_{disk} the outer edge of the accretion disk, and β is a numerical factor showing the degree of thickness. Here, we assume $\beta = 0.01$ during the strong wind phase because the flaring-up edge of the accretion disk is blown in the wind, but it increases to $\beta = 0.15$ after the wind stops (Schandl et al. 1997). The surface of the accretion disk is divided into 16 pieces logarithmically in the radial direction and into 32 pieces evenly in the azimuthal angle as shown in Figure 1. The outer edge of the accretion disk is also divided into 32 pieces by rectangles.

The luminosity of the accretion disk depends strongly on both the thickness of β and the radius of R_{disk} . The size of the accretion disk is also assumed to be given by

$$R_{\text{disk}} = \alpha R_1^*, \quad (3)$$

where R_1^* is the effective radius of the inner critical Roche lobe given by Eggleton's (1983) formula. The viscous heating is neglected because it is rather smaller than that of the irradiation effects.

We assume that the disk is tilting due to Pringle's (1996) mechanism. The tilting disk is introduced by inclining the above disk by degree of $i_{\text{prec}} = 35^\circ$ with a precessing angular velocity of

$$\Omega_{\text{prec}} = \gamma \Omega_{\text{orb}}. \quad (4)$$

The initial phase of precession is assumed to be $\phi_0 = -170^\circ$ at the epoch of spectroscopic conjunction with the M-giant in front, i.e., JD 243 1931.05 + 227.67 E at $E = 0$ (Lines et al. 1988).

3. RESULTS

To fit the first peak of the outburst light curve, we have calculated four cases of V -magnitude light curves with four different WD masses, i.e., $M_{\text{WD}} = 1.377 M_{\odot}$, $1.35 M_{\odot}$, $1.3 M_{\odot}$, and $1.2 M_{\odot}$ and found that both the $1.377 M_{\odot}$ and $1.35 M_{\odot}$ light curves are in much better agreement with the observational one than the other less massive ones as already shown by Kato (1995, 1999). Therefore, we adopt the $M_{\text{WD}} = 1.35 M_{\odot}$ in this Letter.

The optically thick wind stops about 100 days after the luminosity peak, around 1960 (JD 2430000+) as shown in Figure 2. Here, we assume that the mass accretion rate (\dot{M}_{acc}) to the WD is increased to a few times $10^{-7} M_{\odot} \text{ yr}^{-1}$, because the disk is heated up by the WD photosphere (also once engulfed by the WD photosphere). The hydrogen shell-burning vanishes 120 days after the peak when $\dot{M}_{\text{acc}} < 1 \times 10^{-7} M_{\odot} \text{ yr}^{-1}$, while it continues for rather long period when $\dot{M}_{\text{acc}} > 4 \times 10^{-7} M_{\odot} \text{ yr}^{-1}$ as shown in Table 1.

The upper panel in Figure 2 shows the theoretical V -magnitude light curve (solid line) of the WD photosphere with $\dot{M}_{\text{acc}} = 4 \times 10^{-7} M_{\odot} \text{ yr}^{-1}$ and the companion without irradiation together with the observational points (open circles; taken from Pettit 1946a, b, c, d). Two arrows indicate epochs of the spectroscopic conjunction with the M-giant in front (Lines et al. 1988). The ellipsoidal light variation is clearly shown in the later phase. The second panel depicts the V -magnitude including the effects of the companion irradiated by the WD. As already suggested

by Webbink et al. (1987), this cannot well reproduce the second peak of the light curves. The third panel shows the theoretical light curve further including the tilting accretion disk irradiated by the WD photosphere. It fully reproduces the observational light curve if we choose the fitting parameters of $\alpha = 0.7$, $\beta = 0.15$, $\gamma = 9/8$, $i_{\text{prec}} = 35^\circ$, and $\phi_0 = -170^\circ$.

4. DISCUSSION

The radiation induced instability of the accretion disk sets in if the condition

$$\frac{\dot{M}_{\text{acc}}}{1 \times 10^{-7} M_{\odot} \text{ yr}^{-1}} \lesssim 2 \left(\frac{R_{\text{disk}}}{50 R_{\odot}} \right)^{1/2} \left(\frac{L_{\text{bol}}}{2 \times 10^{38} \text{ erg s}^{-1}} \right) \times \left(\frac{R_{\text{WD}}}{0.004 R_{\odot}} \right)^{1/2} \left(\frac{M_{\text{WD}}}{1.35 M_{\odot}} \right)^{-1/2} \quad (5)$$

is satisfied (Southwell et al. 1997). Selvelli et al. (1992) estimated the accretion rate of T CrB as $\dot{M}_{\text{acc}} \sim 0.25 \times 10^{-7} M_{\odot} \text{ yr}^{-1}$, which meets condition (5). Therefore, we can expect the radiation induced instability in T CrB system. The growth timescale of warping is estimated by Pringle (1996) and Livio & Pringle (1996) as the same timescale of the precessing period, i.e.,

$$\tau_{\text{prec}} \simeq 40 \left(\frac{M_{\text{disk}}}{1 \times 10^{-6} M_{\odot}} \right) \left(\frac{R_{\text{disk}}}{50 R_{\odot}} \right) \times \left(\frac{P_{\text{orb}}}{223 \text{ day}} \right)^{-1} \left(\frac{L_{\text{bol}}}{2 \times 10^{38} \text{ erg s}^{-1}} \right)^{-1} \text{ day}, \quad (6)$$

where we assume that the α -parameter of the standard accretion disk is $\alpha \sim 0.1$. Thus, the growth timescale is short enough to excite warping of the accretion disk. It should be noted here that the heated accretion disk surface, just after the maximum expansion of the WD photosphere, could drive a disk wind because the disk has once been engulfed by the WD photosphere. Such a wind could exert an even larger back pressure on the disk than radiation and thus lead to tilting (e.g., Schandl & Meyer 1994; Schandl 1996). Its growth timescale is much shorter than the timescale given by equation (6).

The large inclination angle of the accretion disk such as $i_{\text{prec}} \sim 30 - 35^\circ$ is required to reproduce the observational light curve mainly because we need a reflection area as large as the companion, which is viewed from ours as shown in Figure 1. About 10% faster precessing angular velocity is also required from the phase relation between the rising shoulder of the second peak near 1970 (JD 2430000+), a small dip near 2100 JD, and then a small bump near 2130 JD as shown in Figure 2. These dips are caused by a large shadow on the companion cast by the accretion disk. This precession velocity is consistent with the fact that the radiation-induced precession is prograde, while the tidally induced precession is retrograde.

This research has been supported in part by the Grant-in-Aid for Scientific Research (08640321, 09640325) of the Japanese Ministry of Education, Science, Culture, and Sports.

REFERENCES

Allen, C. W. 1973, in *Astrophysical Quantities* (London: The Athlone Press), chap. 10

Belczyński, K., & Mikolajewska, J. 1998, MNRAS, 296, 77

Cannizzo, J. K., & Kenyon, S. J. 1992, ApJ, 386, L17

Eggleton, P. P. 1983, ApJ, 268, 368

Iglesias, C. A., & Rogers, F. 1996, ApJ, 464, 943

Kato, M. 1995, in *Cataclysmic Variables*, eds. A. Bianchini, M. Della Valle, & M. Orio (Dordrecht: Kluwer), 243

Kato, M. 1999, ApJS, submitted

Kato, M., & Hachisu, I., 1994, ApJ, 437, 802

Leibowitz, E. M., Ofek, E. O., & Mattei, J. A. 1997, MNRAS, 287, 634

Lines, H. C., Lines, R. D., & McFaul, T. G. 1988, AJ, 95, 1505

Livio, M., & Pringle, J. E. 1996, ApJ, 465, L55

Nomoto, K., Thielemann, F., & Yokoi, K. 1984, ApJ, 286, 644

Pettit, E. 1946a, PASP, 58, 153

Pettit, E. 1946b, PASP, 58, 213

Pettit, E. 1946c, PASP, 58, 255

Pettit, E. 1946d, PASP, 58, 359

Pringle, J. E. 1996, MNRAS, 281, 357

Rogers, F. J., & Iglesias, C. A., 1992, ApJS, 79, 507

Ruffert, M., Cannizzo, J. K., & Kenyon, S. J. 1993, ApJ, 419, 780

Schandl, S. 1996, A&A, 307, 95

Schandl, S., & Meyer, F. 1994, A&A, 289, 149

Schandl, S., Meyer-Hofmeister, E., & Meyer, F. 1997, A&A, 318, 73

Selvelli, P. L., Cassatella, A., & Gilmozzi, R. 1992, ApJ, 393, 289

Shahbaz, T., Somers, M., Yudin, B., & Naylor, T. 1992, MNRAS, 288, 1027

Southwell, K. A., Livio, M., & Pringle, J. E. 1997, ApJ, 478, L29

Webbink, R. F. 1976, Nature, 262, 271

Webbink, R. F., Livio, M., Truran, J. W., & Orio, M. 1987, ApJ, 314, 653

Wilson, R. E. 1990, ApJ, 356, 613

TABLE 1
PERIODS OF WIND AND NUCLEAR BURNING PHASES AFTER THE PEAK.

\dot{M}_{acc} ($10^{-7} M_{\odot} \text{ yr}^{-1}$)	wind phase (day)	H-burning (day)
0.0	75	111
1.0	78	121
2.0	82	135
4.0	93	∞

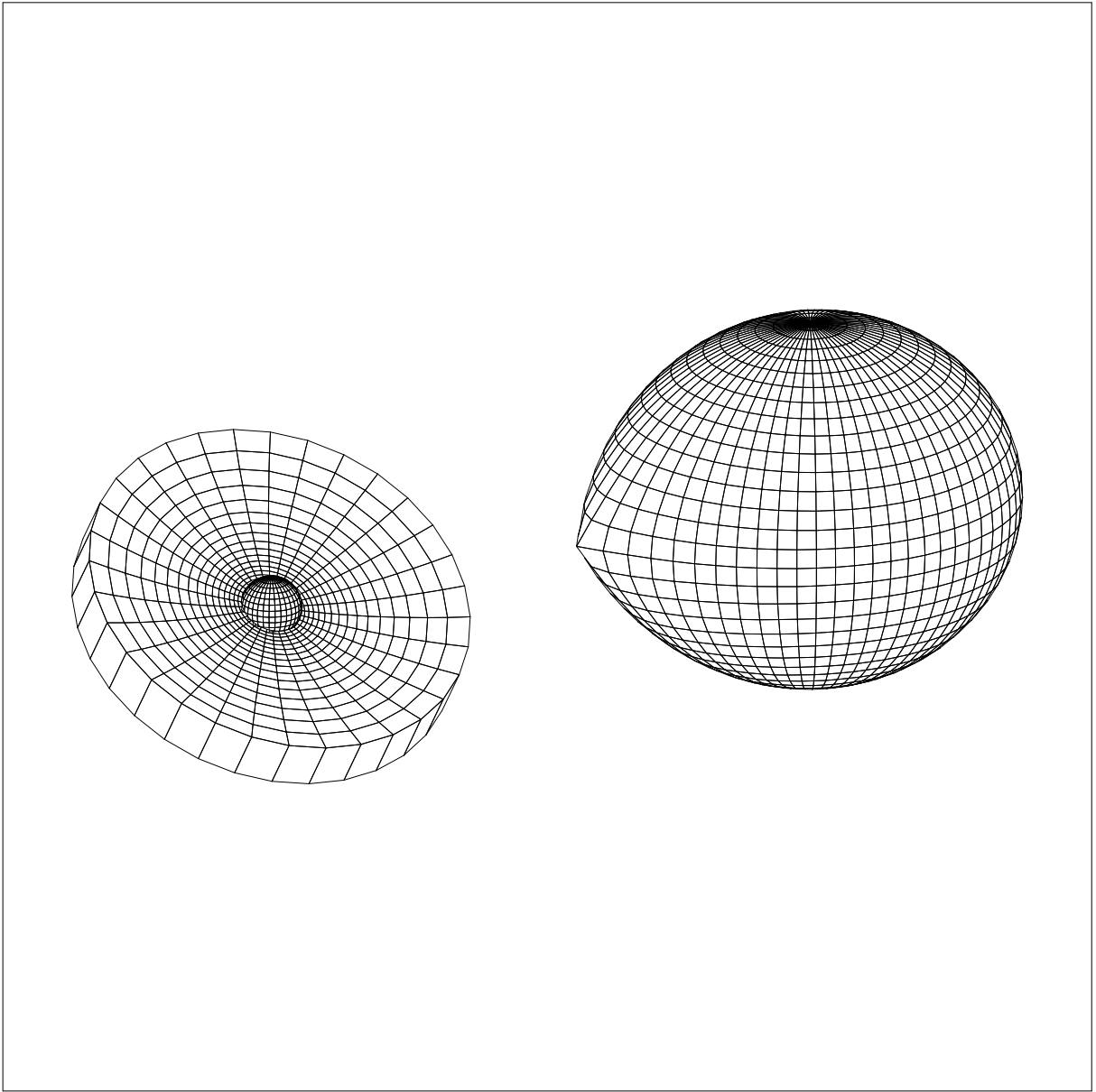


FIG. 1.— Model configuration near the second peak of the recurrent nova T CrB. The cool component (right in the figure) is a red-giant filling up its inner critical Roche lobe. The hemisphere is heated up by the hot component ($1.35 M_{\odot}$ white dwarf, left in the figure). We assume a tilting accretion disk around the hot component, which is precessing about 10% faster than the orbital rotation. The surface of the accretion disk is also heated up by the hot component. The photospheric radius of the hot component near the second peak is as small as $\sim 0.05 R_{\odot}$, about ~ 0.001 times the size of the cool component, but it is exaggerated in this figure to easily see it.

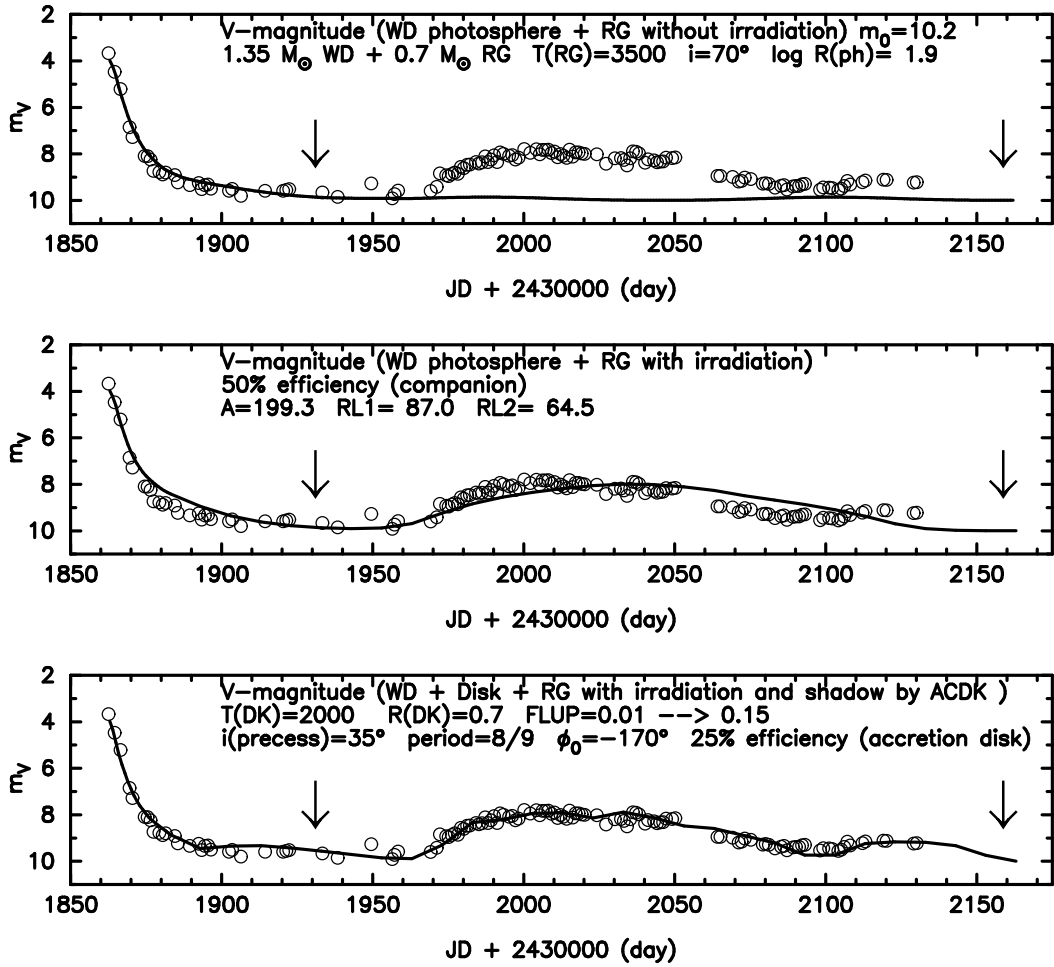


FIG. 2.— Model light curves are plotted against time (JD 2430000+) together with the observational points (Pettit 1946a, 1946b, 1946c, 1946d). Top panel: the visual magnitude of the sum of the white dwarf (WD) photosphere and the red giant (RG) photosphere without irradiation. Middle panel: the visual magnitude of the WD photosphere and the RG photosphere with irradiation. Bottom panel: the visual magnitude of the WD, RG with irradiation, and the accretion disk heated-up by the hot component.